

WORK PACKAGES 8-11 (MSCO₂)

4. Scientific and technical performance

4.2 Overview of Technical Progress

Main Results:

- 3D identification of CO₂ distribution from seismic.
- Development of an initial depth model derived from the seismic velocities.
- Development of a coarsened version of the reservoir flow model obtained from SINTEF, resulting in a significantly reduced run time.
- Development of a procedure for updating the existing reservoir flow model geometry to a model consistent with the depth model of the seismic.

WP 8

A 3D blind deconvolution algorithm, returning both a wavelet and an estimate of the discrete reflectivity series of the Utsira formation, has been applied on both the 1994 and the 1999 seismic data sets. This, together with the identified CO₂ distribution has resulted in an initial model of the Utsira formation.

An initial interval velocity model has been derived, and a post-stack time-to-depth conversion of the 1994 seismic was performed.

WP 9

The 3D distribution of CO₂ has been identified from the first time lapse survey, by applying an automatic approach of finding the envelope of the seismic signal, filtering this in the horizontal directions and then applying a threshold to the values. A particular view of this distribution is depicted in Figure 3. The top and base Utsira horizons are shown as green and blue surfaces respectively. An MPEG film has also been created and is attached to this report in electronic format.

WP 11

The reservoir flow model was obtained from Sintef Petroleum Research. The run time of this model on the local computers was around 4 days, and a simplification of the model has been undertaken in order to enable iterative optimisation runs of this. The run time of the coarsened model is now around 40 minutes.

The domain transformation algorithm, which transforms properties from the reservoir flow model into the geophysical work station or vice versa has been developed. An example of the CO₂ cloud derived from the reservoir simulator as seen in the 'seismic domain' is given in Figure 6.

Algorithms have been developed which ensure consistency between the geometry of the reservoir flow model and the time-to-depth converted seismic. The reservoir flow model geometry has been updated according to the time-to-depth converted seismic.

4.3 Comparison of planned work with actual work

More efforts will be put into analysis of the pre-stack seismic data than outlined in the work package description. This is desirable in order to arrive at a better velocity model of the seismic data, and hence in order to arrive at a better depth model of the sub-surface. This may again be applied to the reservoir flow model in order to ensure geometric consistency between the two domains.

4.5 Brief forecast of the next six months activities and work

The work will focus on the pre-stack velocity analysis of the pre-stack seismic data. In addition, efforts will be spent on ensuring geometric consistency between the reservoir flow model and the depth model arrived at from the seismic. Automated optimisation runs will be applied on the reservoir flow model in order to identify the locations of the holes in the horizontal flow barriers (shale layers) in the Utsira formation.

6. Dissemination and Use of results

No dissemination activities have been undertaken in the reporting period.

Annex – Major results from Work Packages 8-11 (MSCO₂)

WP 8. Initial Model.

A 3D blind deconvolution algorithm, returning both a wavelet and an estimate of the discrete reflectivity series of the Utsira formation, has been applied on both the 1994 and the 1999 seismic data sets. This, together with the identified CO₂ distribution has resulted in the initial model of the Utsira formation. The results of this exercise will aid in the reflection analysis of the seismic in terms of determining accurate distributions of CO₂ in the Utsira reservoir.

An initial interval velocity model has been derived using seismic processing software, and a post-stack time-to-depth conversion of the 1994 seismic was performed. Figure 1 shows a seismic section of both the original seismic in two-way-travel time and in depth according to the initial velocity model.

The depth model will be actively used and refined during the next reporting period in order to undertake advanced velocity analysis of the pre-stack seismic data.

WP 9. CO₂ Cloud detection.

In order to compare results from a reservoir simulation model with the 4D seismic, estimates for the position and extent of the gas clouds have to be made directly from the seismic.

Reflection strength based analysis

The seismic survey from 1999 reveals 4-5 strong reflectors positioned in different layers above the injector well. These may be identified by traditional means such as horizon tracking. Here, another approach is applied.

Similar to what is used in medical ultrasound imaging, the reflection strength, or the envelope of the seismic traces are calculated. The effect is seen in Figure 2, where the envelope of the traces in the difference-cube between the 1999 and 1994 surveys is shown. In order to reduce the noise in the image, the envelope cube is filtered in the horizontal directions using a Gaussian low pass filter with pass band equal to 3 samples in both directions. As seen in the figure, the filtered envelope cube reveals rather clearly the different reflection layers in the seismic. Normalized by the initial reflection strength at top Utsira the envelope cube expresses the fractional difference in reflection strength caused by the gas.

If the gas injected in Utsira formed a single gas column, the reflectivity changes caused by the injection could be related directly to saturation changes, see Brevik et al. [1]. According to this model, an increase in CO₂ saturation from 0% to 75% would result in an increase in the reflectivity by approximately a factor of 3. If the gas is captured by impermeable shale layers, the thickness of the gas layer will affect the reflectivity as well. Due to interference between the reflected wave coming from the wavelet entering the gas

layer and the reflected wave coming from the wavelet leaving the layer, the reflectivity will increase approximately linearly with the thickness of the layer for small layer thickness [2]. Since the thickness of the gas layers may be smaller than the vertical resolution of the seismic, it may therefore be difficult to estimate the saturation of gas in the different layers without resorting to complex modeling. However, since the transition from a strong signal to a weaker signal is rather abrupt, the filtered envelope cube may be used to detect whether gas is present or not in a given position. To get an impression of the spatial distribution of the gas, a 3D iso-surface plot corresponding to an increase in reflectivity by a factor of 3 is shown in Figure 3. This figure clearly shows the layered structure of the seismic signal.

In the estimate of the distribution of the CO₂ clouds, a threshold was applied to the envelope cube. The nature of the estimated CO₂ distribution depends on the value of this threshold. Figure 3 shows an image where the third cloud from the bottom changes in size as a result of changing this threshold. Currently, the available models are uncertain with regards to the relationship between an increase in the reflectivity and an increase in the given gas saturation, and hence there will be a large degree of uncertainty associated with the chosen threshold. In the following we assume this threshold to be 3, i.e. the threshold corresponds to an increase in reflectivity by a factor of 3 compared with the original '94 top Utsira reflection. This implies that a thick gas column of at least 75% gas saturation is located under top Utsira.

WP 11. From Seismic to Reservoir Simulation

The Eclipse reservoir model used here was developed by SACS partner SINTEF Petroleum Research and is documented elsewhere. The model consists of 70 x 85 x 72 grid blocks. The grid spacing is equidistant in the horizontal directions with DX x DY = 34.4m x 36.1m. The main geometrical features governing the distribution and flow of the injected gas are the top of the formation and 4 impermeable layers. These layers contain holes, through which the gas may escape upwards. These layers are indicated in Figure 5.

In order to compare the results from the seismic analysis with the computed results from the reservoir flow model, it is a necessity that these domains may be compared in a correct manner. This implies that a transformation algorithm is required that transports properties from the reservoir flow model to the seismic domain, or vice versa. A software tool has been developed which undertakes this task, and an example of a transformation of the reservoir simulation model to the seismic domain is depicted in Figure 6. Here, the CO₂ gas distribution of September 1999 as computed by the reservoir flow model has been transformed in the geophysical work station. This implies that we are now in a position where accurate comparisons may be made between the two domains.

Seismic vs. Simulator predictions

In order to compare the results from the seismic analysis with that of the reservoir flow model, the filtered envelope cube was transformed into the geometry of the reservoir flow model. The five gas clouds were picked out of the seismic. The thresholded layers are thence projected onto a binary, two-dimensional grid, indicating whether gas is present or

not. This grid is then interpolated to a grid having the dimension of the x-y grid in the Eclipse reservoir flow model. Corresponding binary maps were made based on the Eclipse predictions. In this case, the threshold was set at a gas saturation of 75%. The different maps are shown in Figure 7 and Figure 8. The most pronounced difference between the simulation and the interpreted seismic is that in the simulation the gas has not reached the top of the reservoir by September 1999.

Coarsening of reservoir model

The original 70 x 85 x 72 cell model consumed approximately 55 CPU hours on a simulation from 1996 to 2001. In order to be able to optimize this simulation automatically in an iterative optimisation loop, it is imperative to be able to perform faster simulations. The Eclipse keyword COARSEN was used in order to reduce the number of active grid-cells in the model. The coarsening factor in the vertical direction is largest immediately above the shale layers, while there is no coarsening immediately below the layers. The number of active cells in this new model is 20925 which is approximately 1/20 of the original 428400 cell model. The simulation time is now about 40 minutes.

When such a “brutal” coarsening is applied to a model, it is very important to validate the result. Figure 9 shows the distribution of gas beneath the shale layers in the coarse model. Comparing with the original model in Figure 7 it is seen that the gas distribution is very similar in the two cases.

Geometric updating of the reservoir flow model

In order to ensure consistency with the depth migrated seismic, which will be the focus of next reporting period, an algorithm has been developed which updates the geometry of the reservoir flow model in a data consistent manner. A new version of the reservoir flow model has already been obtained and new simulation runs have been executed with satisfactory results.

References

- [1] Ivar Brevik, Ola Eiken, Rob Arts, Erik Lindeberg and Emmanuel Causse, ‘*Expectations and Results from Seismic Monitoring of CO₂ Injection into a Marine Aquifer*’, EAGE 62nd Conference and Technical Exhibition, Glasgow, Scotland, 29 May - 2 June 2000, article B-21.
- [2] Erik Lindeberg, Emmanuel Causse, Amir Ghaderi, ‘*Evaluations of to what extent CO₂ accumulations in the Utsira formations are possible to quantify by seismic by august 1999*’. SINTEF Petroleum Research

Figures

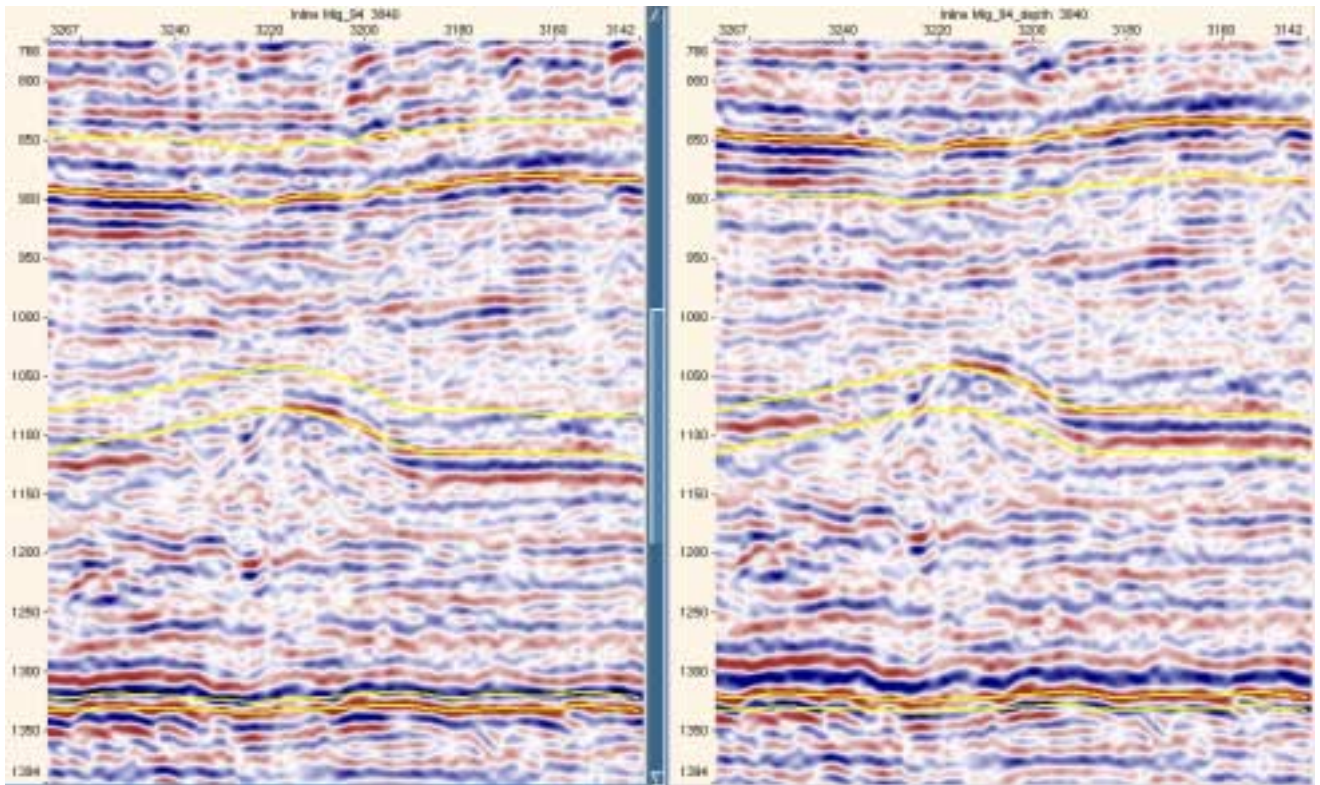


Figure 1. Time-to-Depth Converted seismic (1994 seismic cube).

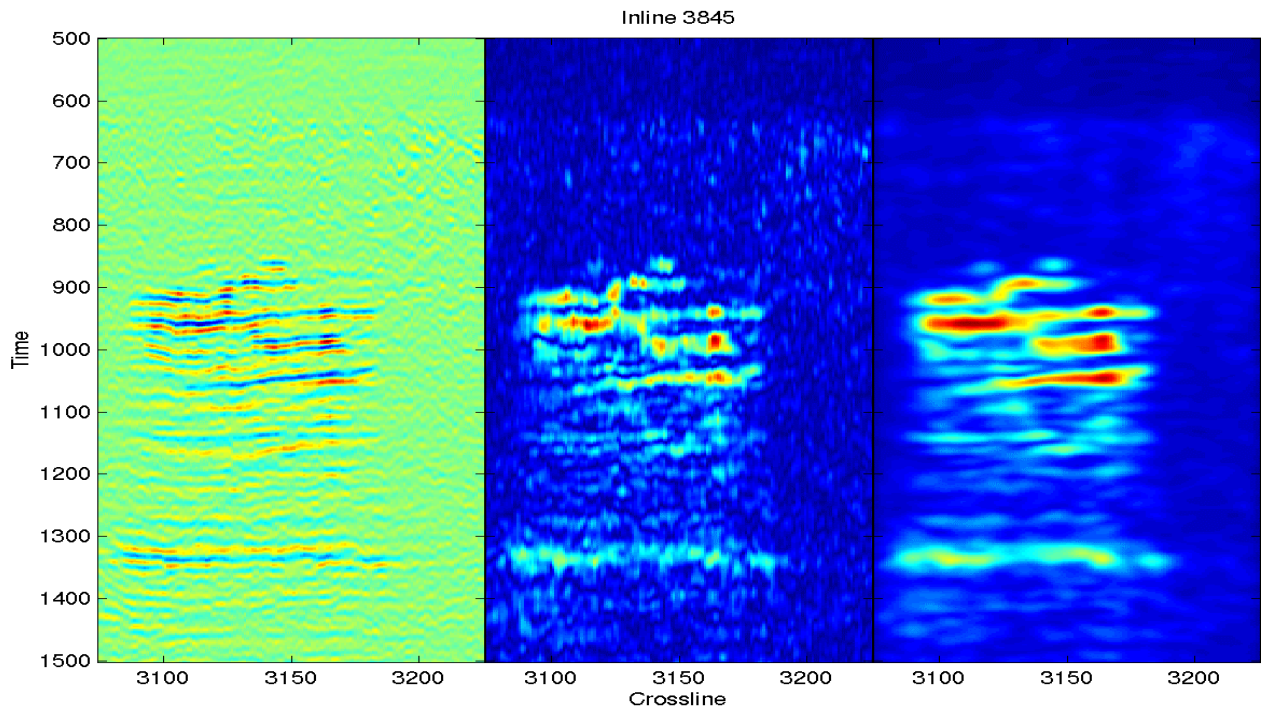


Figure 2. *Left:* Difference cube. *Middle:* Signal envelope cube. *Right:* Gaussian filtered envelope cube.

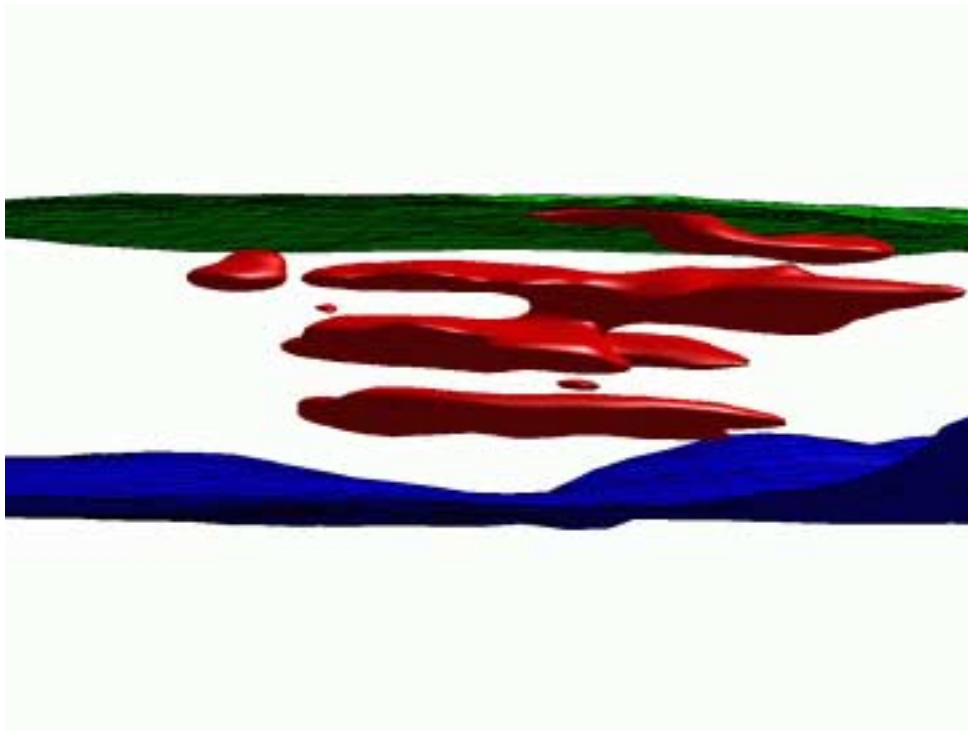


Figure 3. Side view of 3D iso-surfaces of the filtered envelope cube (red). The iso-surfaces correspond to a factor 3 increase in reflectivity compared with the original top Utsira reflection. The green surface is top Utsira and the blue surface is base Utsira.

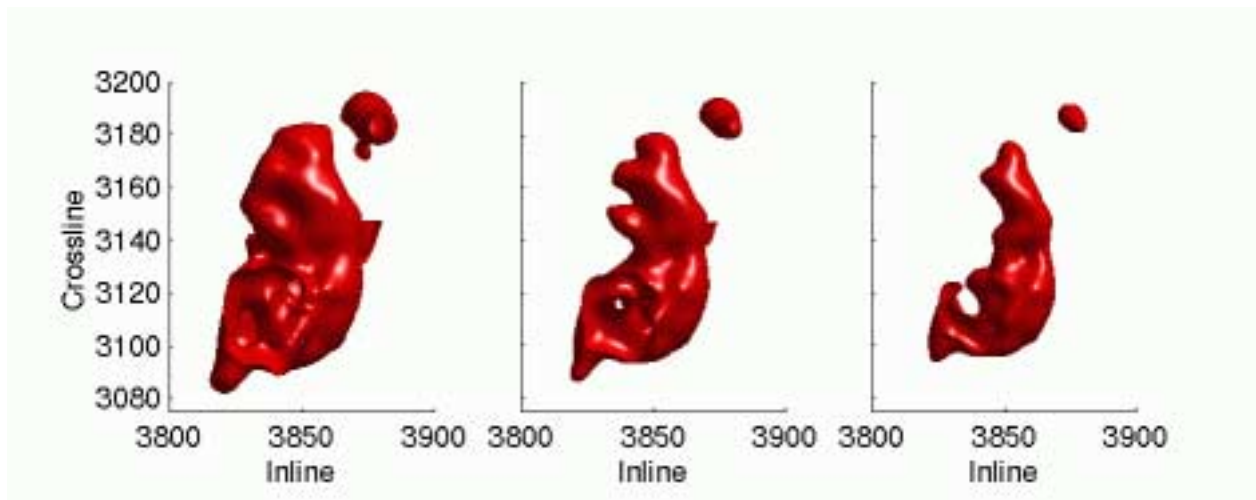


Figure 4. Top view of the third layer. Iso-surfaces of different thresholds in terms of increased reflectivity. Left: factor 2. Middle: factor 3. Right: factor 4.

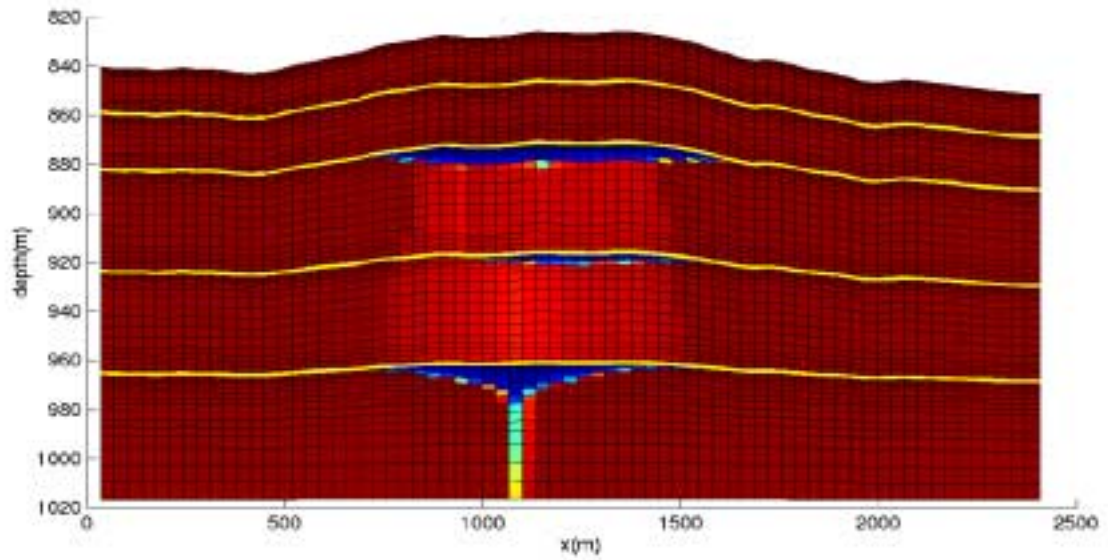


Figure 5. Gas saturation above the injector at September 1999 from the original Eclipse mode. The yellow lines indicate the position of the impermeable shale layers.

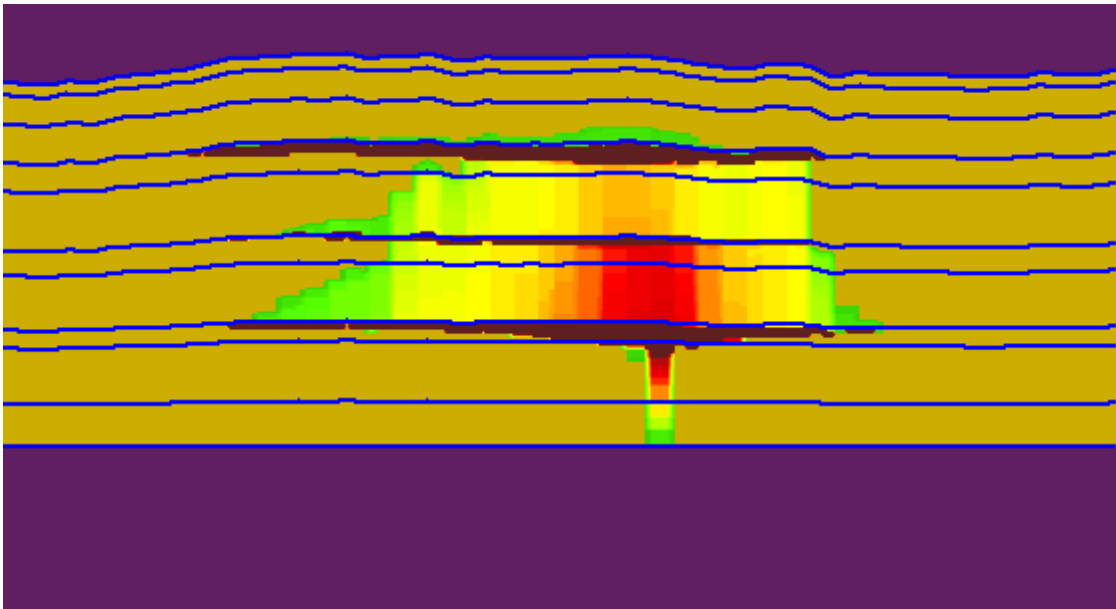


Figure 6. Illustration of the domain transformation algorithm. The computed CO₂ gas distribution from September 1999 is transformed into the seismic interpretation platform.

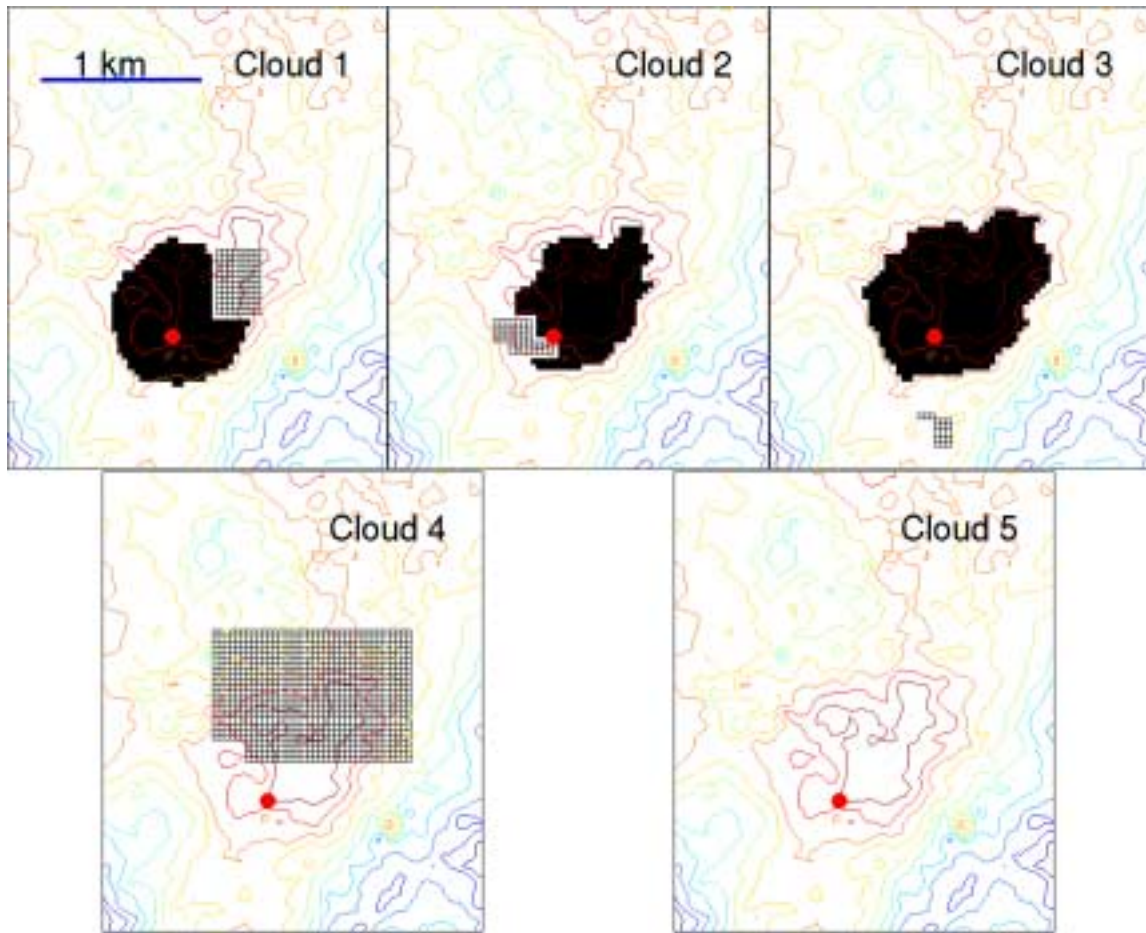


Figure 7. Top view of the gas accumulations september 1999 under the shale layers from the Eclipse simulation. The position of the injector is marked by the red dot. The meshes indicate the openings in the Eclipse model.

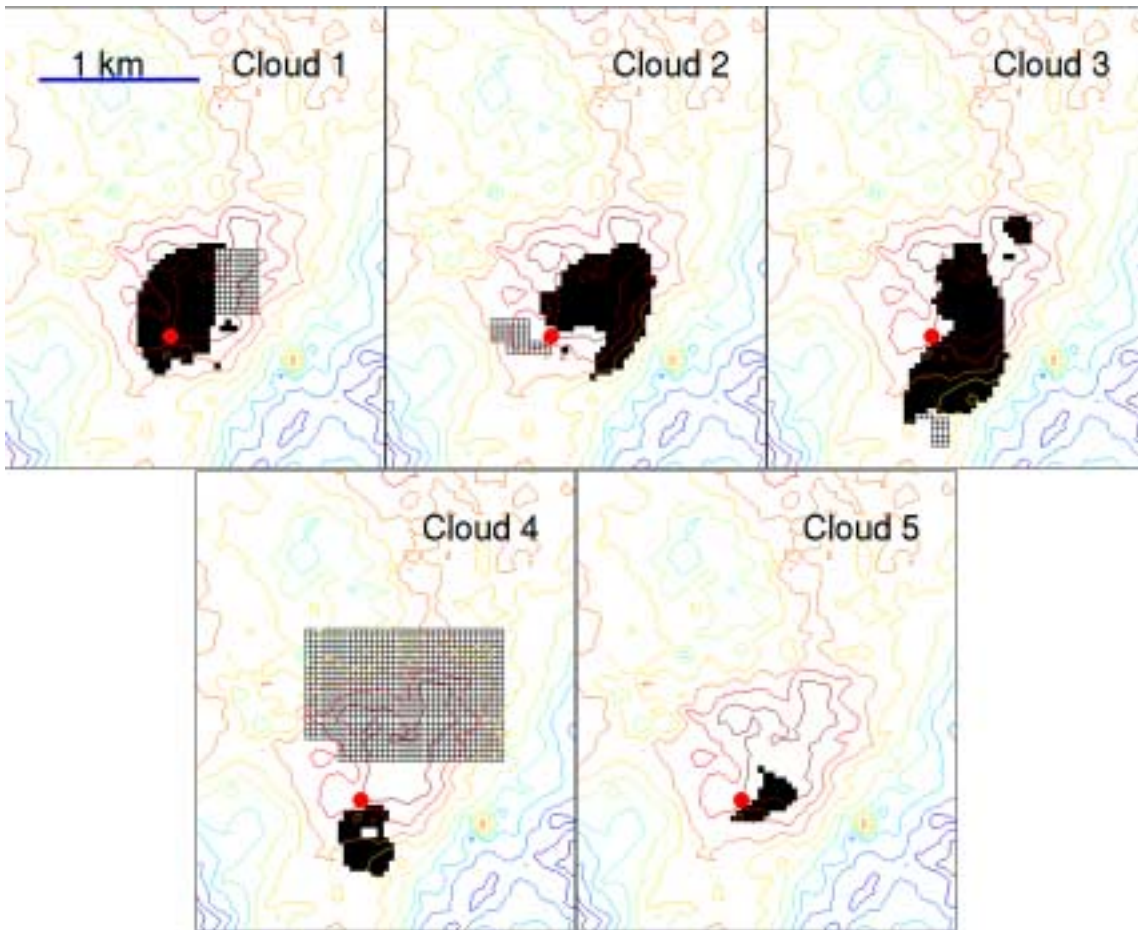


Figure 8. Top view of the interpreted gas clouds form the survey of '99. The position of the injector is marked by the red dot. The meshes indicate the openings in the Eclipse model.

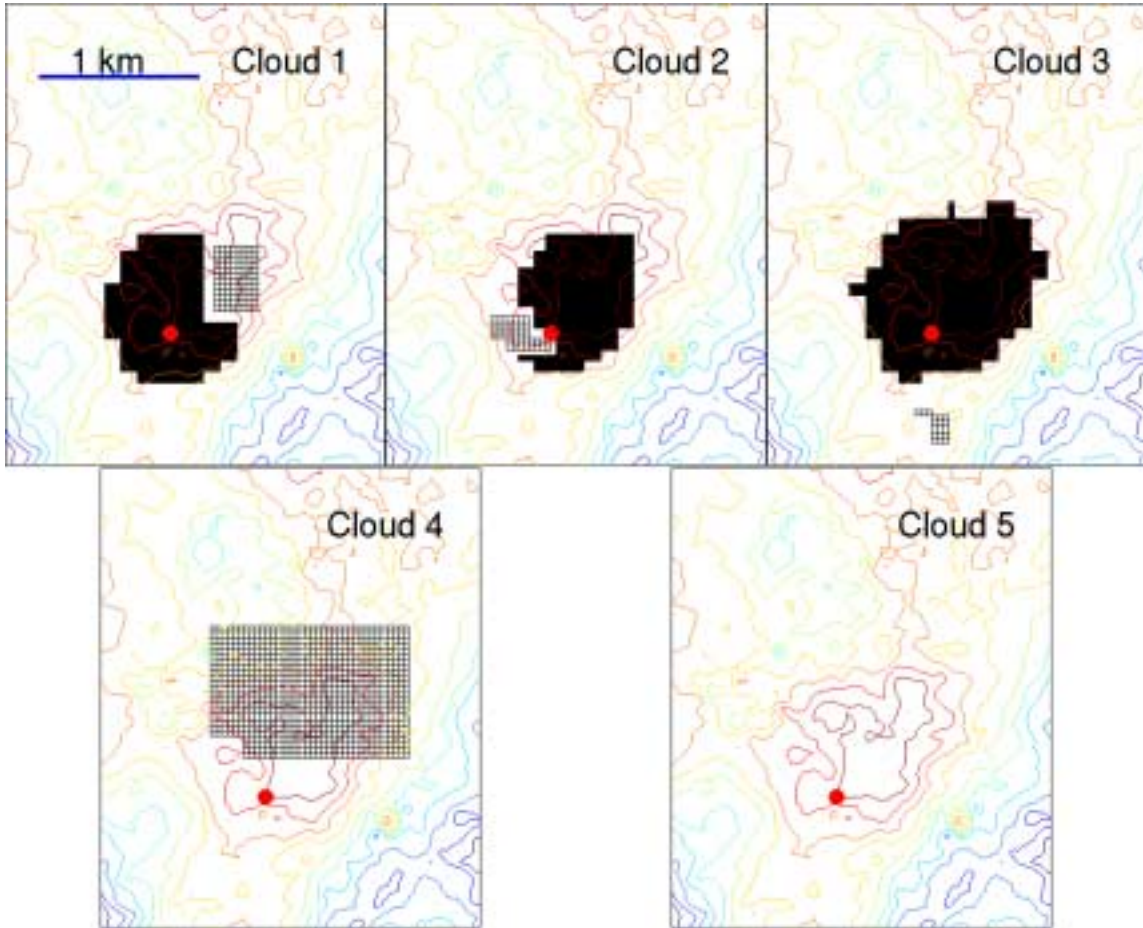


Figure 9. Gas cloud predictions from the coarse 20925-cell model.